



HAL
open science

Clues on the Australasian impact crater site inferred from detailed mineralogical study of a monazite inclusion in a Muong Nong tektite

Anne-Magali Seydoux-Guillaume, P. Rochette, Emmanuel Gardés, Pierre-Marie Zanetta, S. Sao-Joao, Philippe de Parseval, B.P. Glass

► To cite this version:

Anne-Magali Seydoux-Guillaume, P. Rochette, Emmanuel Gardés, Pierre-Marie Zanetta, S. Sao-Joao, et al.. Clues on the Australasian impact crater site inferred from detailed mineralogical study of a monazite inclusion in a Muong Nong tektite. *Geology*, 2024, 109 (9), pp.1578-1590. 10.1130/G52522.1 . hal-04693597

HAL Id: hal-04693597

<https://hal.science/hal-04693597>

Submitted on 10 Sep 2024

HAL is a multi-disciplinary open access archive for the deposit and dissemination of scientific research documents, whether they are published or not. The documents may come from teaching and research institutions in France or abroad, or from public or private research centers.

L'archive ouverte pluridisciplinaire **HAL**, est destinée au dépôt et à la diffusion de documents scientifiques de niveau recherche, publiés ou non, émanant des établissements d'enseignement et de recherche français ou étrangers, des laboratoires publics ou privés.



Distributed under a Creative Commons Attribution 4.0 International License

Clues on the Australasian impact crater site inferred from detailed mineralogical study of a monazite inclusion in a Muong Nong tektite

A.-M. Seydoux-Guillaume^{1,*}, P. Rochette², E. Gardés³, P.-M. Zanetta¹, S. Sao-Joao⁴, Ph. de Parseval⁵, and B.P. Glass⁶

¹Centre National de la Recherche Scientifique (CNRS), Université Jean Monnet Saint-Étienne, Laboratoire de Géologie de Lyon: Terre, Planètes, Environnement (LGL-TPE), UMR5276, F-42023, Saint-Etienne, France

²Aix-Marseille Université, Centre National de la Recherche Scientifique (CNRS), Institut de Recherche pour le Développement (IRD), Institut national de recherche pour l'agriculture, l'alimentation et l'environnement (INRAE), Centre de recherche et d'enseignement des géosciences de l'environnement (CEREGE), UMR7330, F-13545, Aix-en-Provence, France

³Centre National de la Recherche Scientifique (CNRS), Université Clermont Auvergne, Institut de Recherche pour le Développement (IRD), Laboratoire Magmas et Volcans, UMR 6524, F-63170, Aubière, France

⁴Mines Saint-Etienne, Centre National de la Recherche Scientifique (CNRS), Laboratoire Georges Friedel (LGF), UMR 5307, Centre SMS, F-42023, Saint-Etienne, France

⁵Université Toulouse III, Centre National de la Recherche Scientifique (CNRS), Institut de Recherche pour le Développement (IRD), Centre National d'Études Spatiales (CNES), Géosciences Environnement Toulouse/Observatoire Midi-Pyrénées (GET/OMP), UMR 5563, F-31400, Toulouse, France

⁶Department of Geological Sciences, University of Delaware, Newark, Delaware 19716, USA

ABSTRACT

Tektites are terrestrial impact-generated glasses distributed over regions of Earth's surface with ejection distances up to 10,000 km. The Australasian tektite strewn field is the largest and the youngest discovered so far (788 ka). However, the location of the source crater remains unsolved. The present work is the first to investigate the only monazite ever found as an inclusion in a Muong Nong tektite (MNT) from Indochina. In-depth observations down to the nanoscale revealed that the monazite experienced very high temperature, with silicate melt injection sometimes trapped within porosity at the grain boundaries, followed by a recovery mechanism responsible for dislocation migration and subgrain formation. The absence of radiation damage confirms that this recovery episode occurred recently, in line with the age of the tektite. The preservation of a primary zonation (Th component) and the absence of detectable diffusion profiles indicate that the monazite did not reach the melting point (~2050 °C) before initial rapid cooling (~1000 °C/s). The U-Th-total Pb dates of the monazite thus remained unchanged during the impact: 73 ± 6 Ma in a Th-rich domain and 156 ± 15 Ma in a Th-poor domain. This allows the source of the MNT to be constrained. Comparison with a detailed database of monazite ages and Th/U ratios in SE Asia indicates that the Australasian crater should be sought for in the triangle made up of the Philippines, coastal south China, and northern Vietnam, though the latter appears less probable.

INTRODUCTION


Among the terrestrial record of large meteorite impact events (Osinski et al., 2022), a major conundrum remains for the youngest event, which produced the Australasian tektite (AAT) strewn field that ranges from China to Antarctica (Folco et al., 2008; Fig. 1). So far, no crater has been

identified, although the size of the crater has been estimated to be several tens of kilometers based on the study of the ejecta size and distribution (e.g., Glass and Koeberl, 2006). Microtektites are abundant in deep sea sediments and found in association with shocked rock and mineral grains. The distribution of the so-called large, layered Muong Nong tektites (MNTs) points toward Indochina, and more precisely either northeast or southern Indochina, as the possible location of the source

crater (Schnetzler, 1992; Glass and Koeberl, 2006). Based on geophysical and geological considerations, including explanations for the disappearance of the crater under more recent deposits, a source crater location in south and north Indochina was further advocated to be at the Bolaven volcanic plateau (Sieh et al., 2020) and the Red River marine delta (Whymark, 2021), respectively. However, these proposals still lack robust evidence of impact. On the other hand, based mostly on geochemical arguments, Mizera et al. (2016) proposed an alternative area within the source of Chinese loess, namely, the Badain Jaran Desert.

Tektites are relatively homogeneous silica glasses with lechatelierite (pure silica glass) inclusions. Therefore, bulk geochemistry is the primary means of gaining insights into potential target sources. The elemental and isotopic compositions of AATs indicate that the source material would be a continental crust-derived Mesozoic or Quaternary detrital sediment with a Proterozoic parentage (see Blum et al., 1992; review in Mizera et al., 2016). The abundance of ¹⁰Be indicates recent atmospheric contamination, which would be expected from a Quaternary sediment or a soil sequence over older rocks (Ma et al., 2004; Rochette et al., 2018).

MNTs have been shown to record lower temperatures than standard splashform AATs,

A.-M. Seydoux-Guillaume  <https://orcid.org/0000-0002-9921-4695>
*anne.magali.seydoux@univ-st-etienne.fr

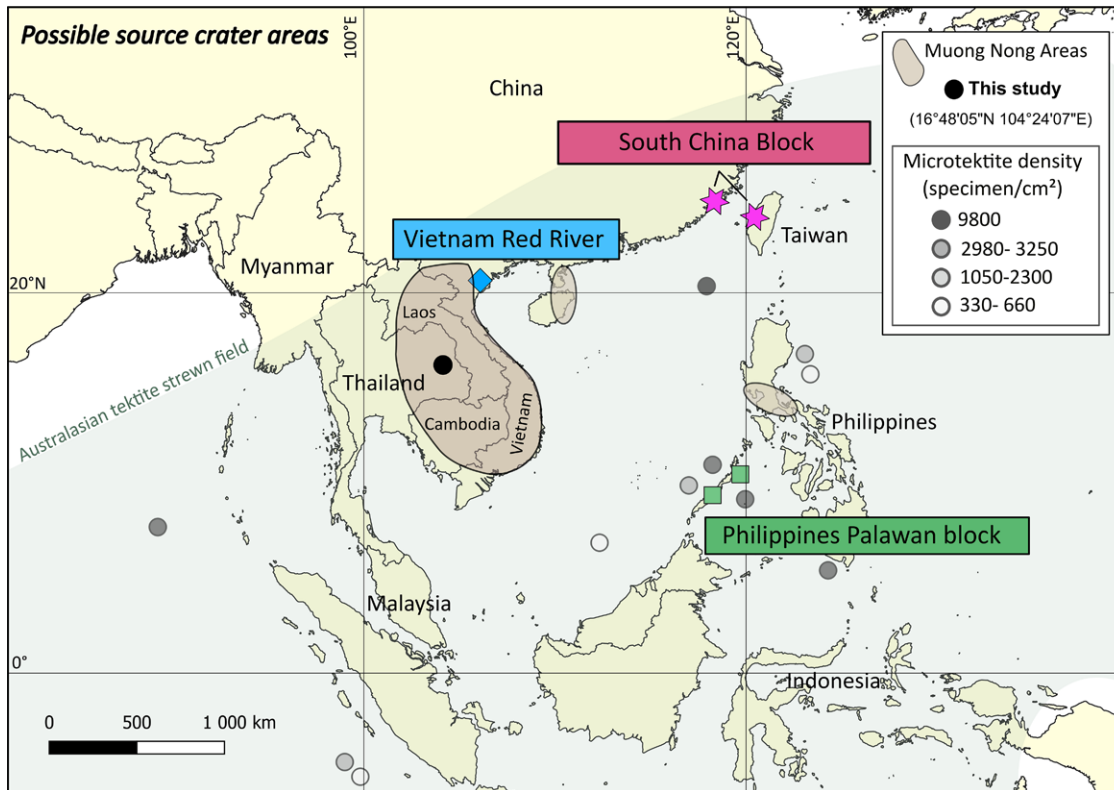


Figure 1. Location of Muong Nong tektites (MNTs) and most probable source crater areas. Most probable source location for monazite inclusion (black circle) analyzed in this study is inferred from Th/U and U-Th–total Pb dates (Fig. 3). Only three main areas ultimately remain (blue, pink, and green symbols): (1) Philippines Palawan block; (2) Vietnam Red River; and (3) South China block.

supporting the hypothesis that the crater resides within or close to the MNT area (Mizote et al., 2003). Probably due to these lower temperatures, MNTs often contain various mineral inclusions (Glass and Barlow, 1979) that can be used as further proxies for the source of the AAT strewn field. Zircon and monazite are widely used to detect the sources of detrital materials due to their ability to preserve the record of their crystallization age over the long term (Mulder and Cawood, 2021). Zircons retrieved by Glass and Barlow (1979) from AATs have been studied by Deloule et al. (2001) and Cavosie et al. (2018). Unfortunately, the isotopic studies of these recrystallized zircons revealed that their isotopic system has been totally reset by impact. Monazite has previously been successfully used to date and constrain complex geological histories, in particular, high-temperature (e.g., Seydoux-Guillaume et al., 2019; Turuani et al., 2022) and impact events (e.g., Erickson et al., 2017, 2020; Kovaleva et al., 2023; Fougereuse et al., 2021; Hyde et al., 2024).

The present work investigates for the first time the only monazite inclusion ever found in an MNT, first discovered by Glass (1972). Based on characterizations down to the nanoscale, we show that its age was not reset during the impact, and we provide new constraints on the thermal history of the MNT-AAT and the location of the source crater.

SAMPLE AND METHODS

The monazite inclusion was isolated by heavy liquid separation after crushing an

MNT sample from east Thailand (Glass, 1972; Fig. 1). The sample is a fragment consisting of a monazite inclusion, identified by X-ray diffraction, surrounded by a thin residue of host glass, both embedded in epoxy and polished (Fig. S1A in the Supplemental Material¹). Characterization of the monazite inclusion was conducted successively with a field emission gun (FEG) scanning electron microscope (SEM), an electron probe micro-analyzer (EPMA), a spherical aberration (Cs)–corrected scanning

¹Supplemental Material. Text S1: Sample provenance, methods, processing, and constraints on the thermal history of the Muong Nong tektite (MNT); Text S2: Complementary zircon data and statistical processing of the monazite database; Figure S1: Additional SEM-TEM images of monazite; Figure S2: EDS-STEM in one pore; Figure S3: Transmission Kikuchi diffraction (TKD) performed on the ion-thinned lamella; Figure S4: Compositional variation diagram (Th + U + Si + Pb) vs. (light rare earth elements [LREEs] + Y + P); Figure S5: EPMA concentration profiles in the glass at the contact with monazite; Figure S6: Final heating rate and initial cooling rate during the MNT thermal event as a function of peak temperature; Figure S7: EDS-SEM maps and line profile across the interface between the Th-rich domain 1 and Th-poor domain 2 within the monazite; Figure S8: Date (U-Th–total Pb) vs. Th/U diagram and sorting of the database; Table S1A: Electron microprobe analyses of monazite; Table S1B: Line scan across monazite-glass interface; Table S2A: EPMA U-Th–total Pb dates with localization and weighted histogram; Table S2B: Isochron-like diagram; and Table S3: Database used for plotting dates (U-Th–total Pb) vs. Th/U diagrams in Figures 4 and S8. Please visit <https://doi.org/10.1130/GEOL.S.26864443> to access the supplemental material; contact editing@geosociety.org with any questions.

transmission electron microscope (STEM), and a transmitted Kikuchi diffraction (TKD) system (see details in Text S1).

RESULTS

Microcharacterization

The monazite (Mnz) inclusion, $60 \times 40 \mu\text{m}$, has a quite rounded shape with a sharp glass-crystal interface (Fig. 2A; Fig. S1A). The border of the inclusion is not smooth but shows a lobate morphology (arrow in inset in Fig. S4). Both chemical mapping (SEM; Fig. 2B; Fig. S7) and electron microprobe point analyses (Fig. S4; Tables S1A and S1B) confirm the presence of a primary zonation (e.g., Th-Mo α -map in Fig. 2B; other elements in Fig. S7) with one domain significantly enriched in thorium (Th) and recording both higher cheralite (Crl) [Ca(Th,U)(PO $_4$) $_2$] and huttonite (Htn) [(Th,U)SiO $_4$] components compared to the other domain (Table S1A; Fig. S4). The transition between both domains is very sharp (Fig. 1B; Fig. S7).

Nanocharacterization

The TKD (Fig. 2C; Fig. S3), annular bright field (ABF)–STEM (Fig. 2D), and bright field (BF) TEM (Fig. S1B) analyses on an ion-thinned lamella revealed that the monazite inclusion is a polycrystal. It is composed of sub-micrometer grains, with misorientation angles $>10^\circ$, and subgrains (200–500 nm), with low-angle boundaries of 2° – 10° formed by variable density of dislocations (Figs. 2C and 2D; Figs. S1B and S3). The monazite contains $\sim 10\%$ porosity with ~ 50 – 800 nm pores, where the largest ones

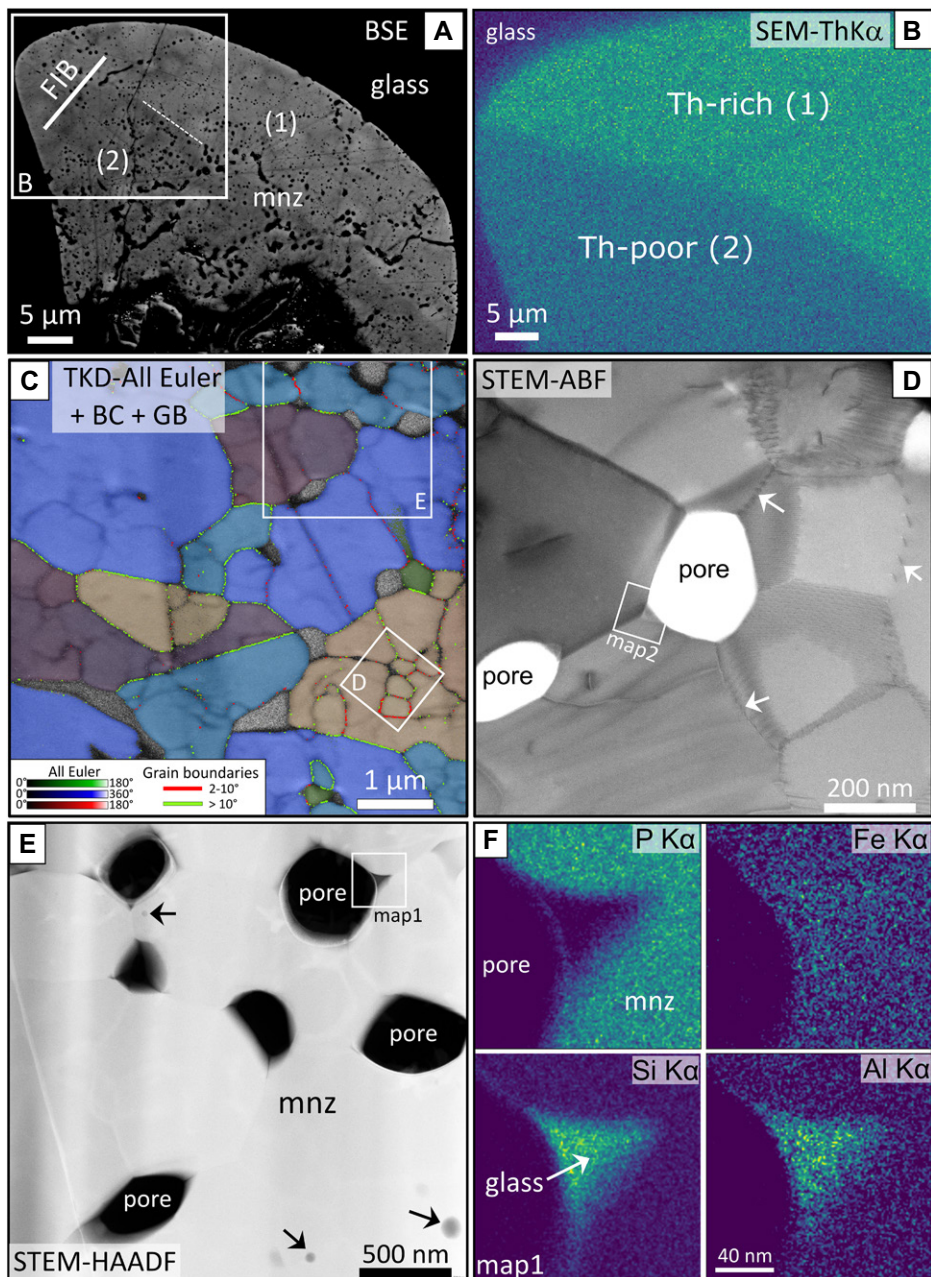


Figure 2. (A–B) Microcharacterization to (C–F) nanocharacterization of monazite inclusion. (A) Backscattered electron (BSE) image of whole monazite (mnz) grain included in tektite glass showing its morphology and zonation and localization of focused ion beam (FIB) foil for transmission electron microscope (TEM) analyses, and energy dispersive X-ray spectrometry (EDS) maps (part B and Fig. S7). (B) Scanning electron microscope (SEM) Th-K α map from part of grain (square in A). (C) Transmission Kikuchi diffraction (TKD) from FIB lamellae. Euler data are superimposed onto grain boundaries and band contrast maps; red—low-angle boundaries (2° – 10°); green—high-angle boundaries ($>10^{\circ}$). Note absence of planar fractures, planar deformation features, deformation twins, and low-strain domains. (D) Annular bright field (ABF) scanning transmission electron microscope (STEM) image. Note presence of pores (white) and subgrains separated by dislocation aligned along low-angle boundaries (arrows). Square (map 2) corresponds to one zone analyzed in Figure S1D (see text footnote 1). (E) High-angle annular dark field (HAADF) STEM images revealing numbers of pores; largest is shown in black, and tiny pores (arrows) are shown in gray (Fig. S2). (F) Chemical mapping (map 1) performed by using EDS in STEM highlights presence of small meniscus of Si- and Al-rich glass in some pores.

(200–800 nm) are always situated at the junctions, sometimes triple junctions, of grain boundaries (Figs. 2C–2E; Figs. S1B and S3). In some cases, bubble walls (a few nanometers thick) were observed as in both upper pores from Figure 2E.

High-angle annular dark field (HAADF) and energy dispersive X-ray spectrometry (EDS)–STEM analyses allow insight into the chemical information (Figs. 2E–2F; Figs. S1D and S2). The sample is homogeneous and does not

present any intragrain variation in composition nor density (homogeneous gray color; Fig. 2E), except for the pores. The monazite is completely free of radiation damage (i.e., no mottled diffraction contrasts in [A]BF-[S]TEM mode in Fig. 2D and Fig. S1B). No evidence of shock deformation features was observed (no planar fractures, planar deformation, deformation twins, or strain domains). Higher magnification (Fig. S1C) and STEM-EDS mapping revealed the presence of a nanometric meniscus of glass enriched in Al, Si, and, to a lesser extent, Fe in some pores at the junction with monazite grains (map 1; Fig. 2F). Across some other grain boundaries (map 2; square in Fig. 2D), enrichment in Fe and S, and depletion in O, was also observed (Fig. S1D).

U–Th–Total Pb Dates

Dates were calculated following the approach of Montel et al. (1996) using the NiLeDAM R-package (Villa-Vialaneix et al., 2013). Dates in Th-rich domain 1 range from 67 Ma to 81 Ma with a mean at 73 ± 6 Ma ($n = 4$). Dates in Th-poor domain 2 range from 140 to 175 Ma with a mean at 156 ± 15 Ma ($n = 4$). Within each domain, no significant date variation was found (Fig. 3; Tables S2A and S2B).

IMPLICATIONS

Constraints on the Thermal History

It appears that the monazite inclusion in the MNT studied here is the relict of a single detrital grain. Its composition (ThO $_2$ > 3 wt% and CaO > 0.6 wt%, $10 < \text{Th/U} > 100$; Table S1A) suggests a magmatic or high-grade ($>500^{\circ}\text{C}$) metamorphic origin (Zi et al., 2024). The absence of radiation damage in this monazite, exposed to a dose of $\sim 5.3 \times 10^{18}$ α/g (Table S2A), implies recent annealing, in line with the age of the MNT (788 ka; Jourdan et al., 2019). For example, a younger (24 Ma) monazite exposed to a dose of $\sim 1.4 \times 10^{18}$ α/g revealed radiation damage (Seydoux-Guillaume et al., 2004). Moreover, it has been experimentally demonstrated that complete healing of radiation damage is attained at 1000°C (Seydoux-Guillaume et al., 2002). The ultrafine-grained structure of the monazite, resulting from short-range dislocation migration, together with pores and traces of silicate glass and iron sulfide indicate rapid recovery at very high temperature. This is in line with previous studies on Australasian MNTs that evidenced peak temperatures higher than 1673°C (Cavosie et al., 2018). However, the preservation of the primary Th zonation and the absence of detectable diffusion profiles ($< \sim 1 \mu\text{m}$) between the two Th domains are consistent with solid-state diffusion over a few nanometers in length, while a liquid state would have implied diffusion a few micrometers in length (Text S1; Figs. S5–S7). Thus, it is most probable that the monazite did not reach its melting point of $\sim 2050^{\circ}\text{C}$ (Hikichi and

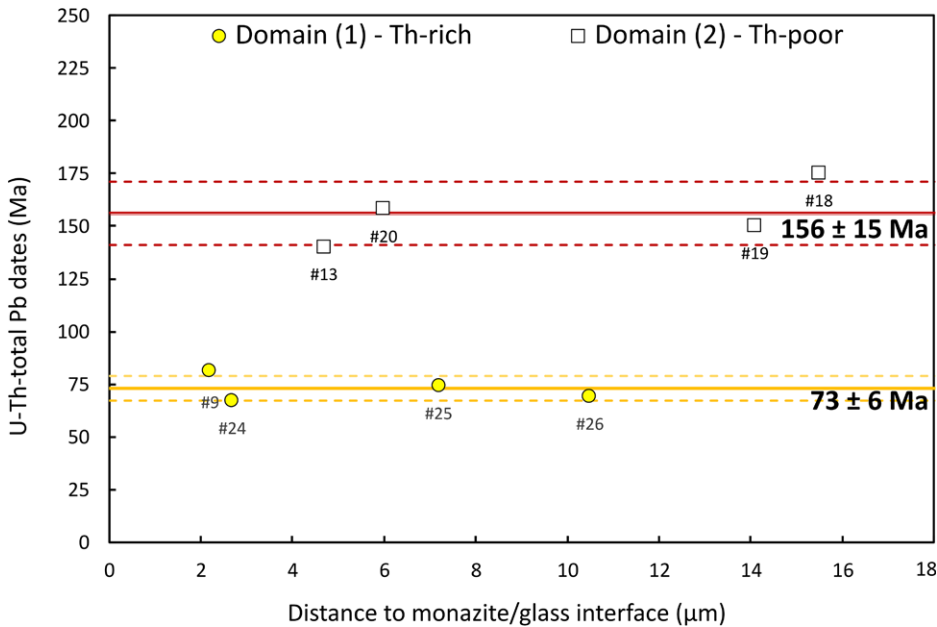


Figure 3. U-Th–total Pb dates represented as function of their distance to monazite/glass interface. Eight dates have been reported from monazite grain. Dates in domain 1 range from 67 ± 17 Ma to 81 ± 22 Ma with mean at 73 ± 6 Ma ($n = 4$). Dates in domain 2 range from 140 ± 44 Ma to 175 ± 31 Ma with mean at 156 ± 15 Ma ($n = 4$) (Table S2A and S2B; see text footnote 1).

Nomura, 1987). Considering the peak temperature was in the 1673–2050 °C range, modeling of the diffusion profiles in silicate melts yielded initial cooling rates broadly around 1000 °C/s (Text S1; Fig. S6). This is in line with the estima-

tion of Masotta et al. (2020). Therefore, because the monazite inclusion did not melt during the impact, and the thermal event was very fast, the dates of the monazite were preserved and can be used as constraints on the source of the MNT.

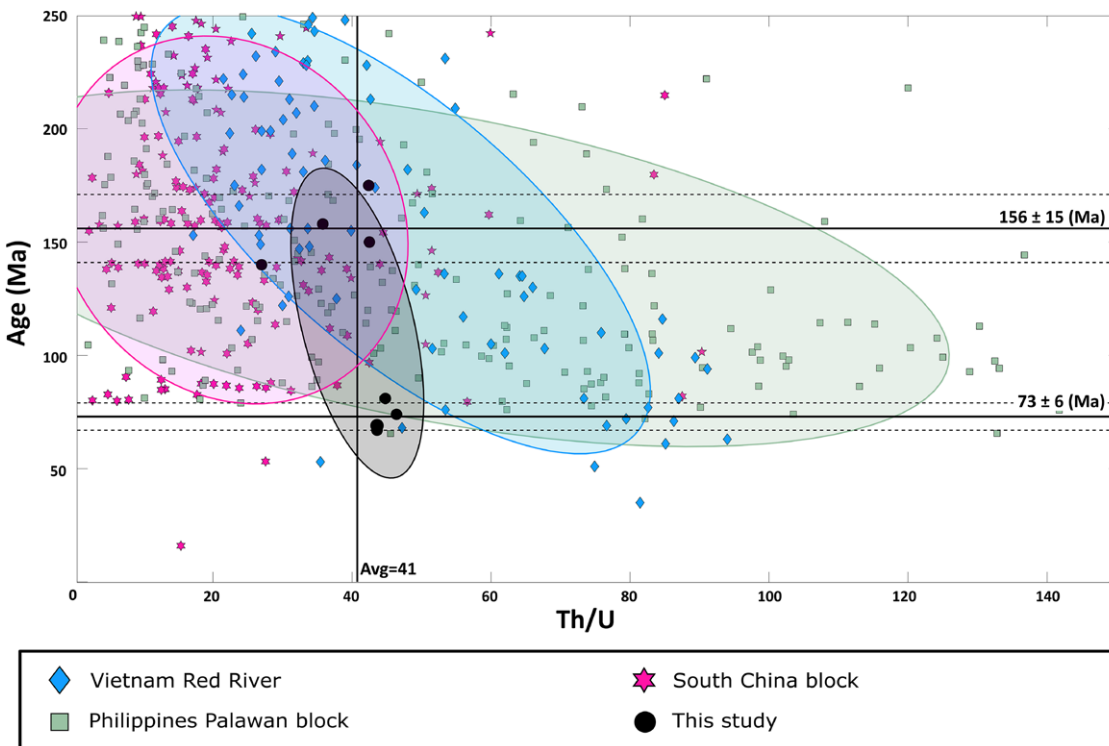


Figure 4. Age (U-Th–total Pb, in Ma) vs. Th/U diagram comparing monazite populations after sorting ($n = 481$) in literature database (Mulder and Cawood, 2021; Nakano et al., 2016) with monazite analyzed in this study. To sort populations, smallest ellipses covering 75% of data points were determined for each population of database. Only populations with ellipsoid that overlapped ellipsoid of data sets from this study (gray oval) were retained (see details in Text S1 and S2 and Fig. S8A; see text footnote 1). Three regions stand out from this statistical comparison: (1) Palawan block in Philippines (Padrones et al., 2017); (2) Red River zone in Vietnam (Nakano et al., 2016); and (3) South China block (Chen et al., 2019). Samples from similar localities (within database) have been regrouped under single denomination (and detailed in Fig. S8B). These localities are shown in Figure 1.

Constraints on the Source of Australasian Tektites

Based on the retained pre-impact dates of the monazite (73 ± 6 Ma and 156 ± 15 Ma), it is possible to constrain the source terrains, and thus the source material. Mulder and Cawood (2021) reported a global compilation of monazite ages ($n > 100,000$), dating methods, locations, and Th and U contents. We used this database, together with the data for northern Vietnam from Nakano et al. (2016), and applied three filters: (1) only EPMA dating methods for consistency with our own data (i.e., U-Th–Pb_{total} dates); (2) dates younger than 250 Ma; to be in the same range as MNT monazite; and (3) locations within 2500 km of the MNT areas (i.e., China, Indonesia, Myanmar, Nepal, Philippines, South Korea, Taiwan, and Vietnam). The ways in which the zircon ages exclude a Mekong watershed or North China impact site are discussed in Text S2. Analyses from the filtered database ($n = 5247$) were plotted in a Th/U versus date diagram (Table S3; Figs. S8A and S8B) and compared with our monazite analyses (Text S1 and S2). Only three locations matched both the ages and the Th/U ratios of the MNT monazite (Figs. 1 and 4): (1) the Palawan block in the Philippines (Padrones et al., 2017), (2) the Red River zone in Vietnam (Nakano et al., 2016), and (3) the South China block (Chen et al., 2019). The Red River zone is commonly reported as a potential source, but the composition of the monazites from this location

(Nakano et al., 2016) strongly differs from the MNT monazite studied here (cheralite component of <0.6 mol% vs. 6–14 mol%, respectively; Table S1A; Fig. S4). While the Red River zone cannot be definitively rejected until chemical data allow the same comparison to be made with monazites from the Palawan and South China blocks, these two locations appear to be more probable candidates for the AAT source crater. As the Palawan and South China blocks were attached ca. 50 Ma, any offshore continental crust in between the two would also fit.

ACKNOWLEDGMENTS

This work was supported by ANR ET-Megafires project (ANR-21-CE49-0014-03). P.-M. Zanetta and A.-M. Seydoux-Guillaume thank the consortium Lyon/Saint Etienne de Microscopies (CLYM) for access to the TEM. We thank Yaya Lefkir and Stéphanie Reynaud (LabHC) for help with the FEG-SEM instrument and for FIB preparation, respectively. Comments by reviewers Axel Wittmann, Elizaveta Kovaleva, and Timmons Erickson, and editor Urs Schaltegger significantly improved the manuscript and are highly appreciated.

REFERENCES CITED

- Blum, J.D., Papanastassiou, D.A., Koeberl, C.A., and Wasserburg, G.J., 1992, Nd and Sr isotopic study of Australasian tektites: New constraints on the provenance and age of target materials: *Geochimica et Cosmochimica Acta*, v. 56, p. 483–492, [https://doi.org/10.1016/0016-7037\(92\)90146-A](https://doi.org/10.1016/0016-7037(92)90146-A).
- Cavosie, A.J., Timms, N.E., Erickson, T.M., and Koeberl, C., 2018, New clues from Earth's most elusive impact crater: Evidence of reidite in Australasian tektites from Thailand: *Geology*, v. 46, p. 203–206, <https://doi.org/10.1130/G39711.1>.
- Chen, C.H., Lee, C.Y., Lin, J.W., and Chu, M.F., 2019, Provenance of sediments in western Foothills and Hsuehshan Range (Taiwan): A new view based on the EMP monazite versus LA-ICPMS zircon geochronology of detrital grains: *Earth-Science Reviews*, v. 190, p. 224–246, <https://doi.org/10.1016/j.earscirev.2018.12.015>.
- Deloule, E., Chaussidon, M., Glass, B.P., and Koeberl, C., 2001, U-Pb isotopic study of relict zircon inclusions recovered from Muong Nong-type tektites: *Geochimica et Cosmochimica Acta*, v. 65, p. 1833–1838, [https://doi.org/10.1016/S0016-7037\(01\)00548-8](https://doi.org/10.1016/S0016-7037(01)00548-8).
- Erickson, T.M., Kirkland, C.L., Timms, N.E., Cavosie, A.J., and Davison, T.M., 2020, Precise radiometric age establishes Yarrabubba, Western Australia, as Earth's oldest recognised meteorite impact structure: *Nature Communications*, v. 11, <https://doi.org/10.1038/s41467-019-13985-7>.
- Erickson, T.M., Timms, N.E., Kirkland, C.L., Tohver, E., Cavosie, A.J., Pearce, M.A., and Reddy, S.M., 2017, Shocked monazite chronometry: Integrating microstructural and in situ isotopic age data for determining precise impact ages: *Contributions to Mineralogy and Petrology*, v. 172, <https://doi.org/10.1007/s00410-017-1328-2>.
- Folco, L., Rochette, P., Perchiazzi, N., D'Orazio, M., Laurenzi, M.A., and Tiepolo, M., 2008, Microtektites from Victoria Land Transantarctic Mountains: *Geology*, v. 36, p. 291–294, <https://doi.org/10.1130/G24528A.1>.
- Fougerouse, D., Cavosie, A.J., Erickson, T., Reddy, S.M., Cox, M.A., Saxey, D.W., Rickard, W.D.A., and Wingate, M.T.D., 2021, A new method for dating impact events—Thermal dependency on nanoscale Pb mobility in monazite shock twins: *Geochimica et Cosmochimica Acta*, v. 314, p. 381–396, <https://doi.org/10.1016/j.gca.2021.08.025>.
- Glass, B.P., 1972, Crystalline inclusions in a Muong Nong-type tektite: *Earth and Planetary Science Letters*, v. 16, p. 23–26, [https://doi.org/10.1016/0012-821X\(72\)90232-4](https://doi.org/10.1016/0012-821X(72)90232-4).
- Glass, B.P., and Barlow, R.A., 1979, Mineral inclusions in Muong Nong-type indochinites: Implications concerning parent material and process of formation: *Meteoritics*, v. 14, p. 55–67, <https://doi.org/10.1111/j.1945-5100.1979.tb00479.x>.
- Glass, B.P., and Koeberl, C., 2006, Australasian microtektites and associated impact ejecta in the South China Sea and the middle Pleistocene supereruption of Toba: *Meteoritics & Planetary Science*, v. 41, p. 305–326, <https://doi.org/10.1111/j.1945-5100.2006.tb00211.x>.
- Hikichi, Y., and Nomura, T., 1987, Melting temperatures of monazite and xenotime: *Journal of the American Ceramic Society*, v. 7, p. 252–253, <https://doi.org/10.1111/j.1151-2916.1987.tb04890.x>.
- Hyde, W.R., Kenny, G.G., Whitehouse, M.J., Wirth, R., Roddatis, V., Schreiber, A., Garde, A.A., Plan, A., and Larsen, N.K., 2024, Microstructural and isotopic analysis of shocked monazite from the Hiawatha impact structure: Development of porosity and its utility in dating impact craters: *Contributions to Mineralogy and Petrology*, v. 179, p. 28, <https://doi.org/10.1007/s00410-024-02097-1>.
- Jourdan, F., Nomade, S., Wingate, M.T.D., Eroglu, E., and Deino, A., 2019, Ultraprecise age and formation temperature of the Australasian tektites constrained by ⁴⁰Ar/³⁹Ar analyses: *Meteoritics & Planetary Science*, v. 54, p. 2573–2591, <https://doi.org/10.1111/maps.13305>.
- Kovaleva, E., Helmy, H., Belkacim, S., Schreiber, A., Wilke, F.D.H., and Wirth, R., 2023, Libyan Desert glass: New evidence for an extremely high pressure-temperature impact event from nanostructural study: *The American Mineralogist*, v. 108, p. 1906–1923, <https://doi.org/10.2138/am-2022-8759>.
- Ma, P., Aggrey, K., Tonzola, C., Schnabel, C., De Nicola, P., Herzog, G.T., Wasson, J.T., Glass, B.P., Brown, L., Tera, F., Middleton, R., and Klein, J., 2004, Beryllium-10 in Australasian tektites: Constraints on the location of the source crater: *Geochimica et Cosmochimica Acta*, v. 68, p. 3883–3896, <https://doi.org/10.1016/j.gca.2004.03.026>.
- Masotta, M., Peres, S., Folco, L., Mancini, L., Rochette, P., Glass, B.P., Campanale, F., Gueninchault, N., Radica, F., Singsoupho, S., and Navarro, E., 2020, 3D tomographic analysis reveals how coesite is preserved in Muong Nong-type tektites: *Scientific Reports*, v. 10, 20608, <https://doi.org/10.1038/s41598-020-76727-6>.
- Mizera, J., Randa, Z., and Kamenik, J., 2016, On a possible parent crater for Australasian tektites: Geochemical, isotopic, geographical and other constraints: *Earth-Science Reviews*, v. 154, p. 123–137, <https://doi.org/10.1016/j.earscirev.2015.12.004>.
- Mizote, S., Matsumoto, T., Matsuda, J., and Koeberl, C., 2003, Noble gases in Muong Nong-type tektites and their implications: *Meteoritics & Planetary Science*, v. 38, p. 747–758, <https://doi.org/10.1111/j.1945-5100.2003.tb00039.x>.
- Montel, J.M., Foret, S., Veschambre, M., Nicollet, C., and Provost, A., 1996, Electron microprobe dating of monazite: *Chemical Geology*, v. 131, p. 37–53, [https://doi.org/10.1016/0009-2541\(96\)00024-1](https://doi.org/10.1016/0009-2541(96)00024-1).
- Mulder, J.A., and Cawood, P.A., 2021, Evaluating preservation bias in the continental growth record against the monazite archive: *Geology*, v. 50, p. 243–247, <https://doi.org/10.1130/G49416.1>.
- Nakano, N., Osanai, Y., Nam, N.V., and Tri, T.V., 2016, Low-temperature eclogite-facies bauxite from the Red River shear zone in Vietnam: Its evolu-

- tion and significance: *Journal of Mineralogical and Petrological Sciences*, v. 111, p. 196–210, <https://doi.org/10.2465/jmps.150727>.
- Osinski, G.R., Grieve, R.A.F., Ferrière, L., Losiak, A., Pickersgill, A.E., Cavosie, A.J., Hibbard, S.M., Hill, P.J.A., Bermudez, J.J., Marion, C.L., and Newman, J.D., 2022, Impact Earth: A review of the terrestrial impact record: *Earth-Science Reviews*, v. 232, <https://doi.org/10.1016/j.earscirev.2022.104112>.
- Padrones, J.T., Tani, K., Tsutsumi, Y., and Imai, A., 2017, Imprints of late Mesozoic tectono-magmatic events on Palawan continental block in northern Palawan, Philippines: *Journal of Asian Earth Sciences*, v. 142, p. 56–76, <https://doi.org/10.1016/j.jseaes.2017.01.027>.
- Rochette, P., Braucher, R., Folco, L., Horng, C.S., Aumaitre, G., Bourlès, D.L., and Keddadouche, K., 2018, ¹⁰Be in Australasian microtektites compared to tektites: Size and geographic controls: *Geology*, v. 46, p. 803–806, <https://doi.org/10.1130/G45038.1>.
- Schnetzler, C.C., 1992, Mechanism of Muong Nong-type tektite formation and speculation on the source of Australasian tektites: *Meteoritics*, v. 27, p. 154–165, <https://doi.org/10.1111/j.1945-5100.1992.tb00743.x>.
- Seydoux-Guillaume, A.-M., Wirth, R., Nasdala, L., Gottschalk, M., Montel, J.-M., and Heinrich, W., 2002, An XRD, TEM and Raman study of experimentally annealed natural monazite: *Physics and Chemistry of Minerals*, v. 29, p. 240–253, <https://doi.org/10.1007/s00269-001-0232-4>.
- Seydoux-Guillaume, A.-M., Wirth, R., Deutsch, A., and Schärer, U., 2004, Microstructure of 24–1928 Ma concordant monazites: Implications for geochronology and nuclear waste deposits: *Geochimica et Cosmochimica Acta*, v. 68, p. 2517–2527, <https://doi.org/10.1016/j.gca.2003.10.042>.
- Seydoux-Guillaume, A.-M., Fougerouse, D., Laurent, A.T., Gardes, E., Reddy, S.M., and Saxey, D.W., 2019, Nanoscale resetting of the Th/Pb system in an isotopically-closed monazite grain: A combined atom probe and transmission electron microscopy study: *Geoscience Frontiers*, v. 10, p. 65–76, <https://doi.org/10.1016/j.gsf.2018.09.004>.
- Sieh, K., Herrin, J., Jicha, B., Angel, D.S., Moore, J.D.P., Banerjee, P., Wiwegwin, W., Sihavong, V., Singer, B., Chualaowanich, T., and Charusiri, P., 2020, Australasian impact crater buried under the Bolaven volcanic field, southern Laos: *Proceedings of the National Academy of Sciences of the United States of America*, v. 12, <https://doi.org/10.1073/pnas.1904368116>.
- Turuani, M.J., Laurent, A.T., Seydoux-Guillaume, A.-M., Fougerouse, D., Saxey, D., Reddy, S.M., Harley, S.L., Reynaud, S., and Rickard, W.D.A., 2022, Partial retention of radiogenic Pb in galena nanocrystals explains discordance in monazite from Napier Complex (Antarctica): *Earth and Planetary Science Letters*, v. 588, <https://doi.org/10.1016/j.epsl.2022.117567>.
- Villa-Vialaneix, N., Montel, J.-M., and Seydoux-Guillaume, A.-M., 2013, NiLeDAM: Monazite data for the NiLeDAM team. R package version 0.1: <https://tuxette.shinyapps.io/NiLeDAM/> (last accessed August 2024).
- Whymark, A., 2021, A review of evidence for a Gulf of Tonkin location for the Australasian tektite source crater: *Thai Geoscience Journal*, v. 2, p. 1–29, <https://doi.org/10.14456/tgj.2021.2>.
- Zi, J.-W., Muhling, J.R., and Rasmussen, B., 2024, Geochemistry of low-temperature (<350 °C) metamorphic and hydrothermal monazite: *Earth-Science Reviews*, v. 249, <https://doi.org/10.1016/j.earscirev.2023.104668>.

Printed in the USA